

# The Role of Reactive Nitrogen Species in Sensitized Photolysis of Wastewater-Derived Trace Organic Contaminants

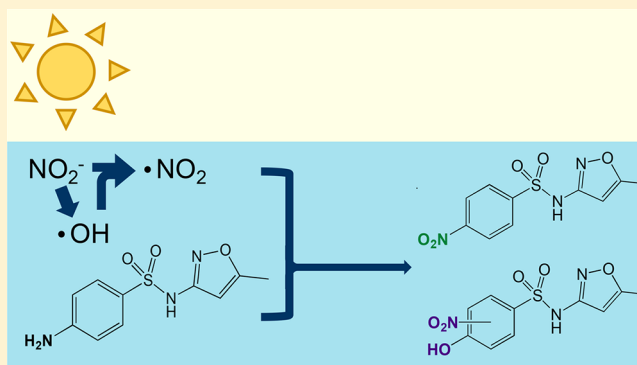
Rachel C. Scholes,<sup>†,‡,§</sup> Carsten Prasse,<sup>†,‡,§</sup> and David L. Sedlak<sup>\*,†,‡,§</sup>

<sup>†</sup>Department of Civil and Environmental Engineering, University of California, Berkeley, California 94720, United States

<sup>‡</sup>NSF Engineering Research Center for Reinventing the Nation's Urban Water Infrastructure (ReNUWIt), Berkeley, California 94720, United States

**S** Supporting Information

**ABSTRACT:** Under conditions typically encountered in the aquatic environment, the absorption of sunlight by nitrite and nitrate leads to the transformation of trace organic contaminants. In addition to the well understood mechanism through which hydroxyl radical ( $\cdot\text{OH}$ ) produced by nitrate and nitrite photolysis oxidizes contaminants, absorption of light also results in the formation of reactive nitrogen species that transform organic contaminants. To assess the importance of this process on the fate of trace organic contaminants, radical quenchers and transformation product analysis were used to discriminate among potential reaction pathways. For sulfamethoxazole, an antibiotic that is frequently detected in municipal wastewater effluent, nitrate and nitrite-sensitized photolysis pathways resulted in production of transformation products that were not detected during direct photolysis or reaction with  $\cdot\text{OH}$ . The reactivity of sulfamethoxazole with the reactive species produced when nitrite absorbed sunlight was affected by the presence of hydroxyl radical scavengers, indicating the likely involvement of nitrogen dioxide, which forms when nitrite reacts with hydroxyl radical. Reactive nitrogen species also reacted with emtricitabine, propranolol, and other trace organic contaminants commonly detected in wastewater effluent, indicating the potential importance of this process to the fate of other trace organic contaminants. A kinetic model indicated that reactive nitrogen species could be important to the phototransformation of trace organic contaminants when relatively high concentrations of nitrite are present (e.g., in surface waters receiving reverse osmosis concentrate from potable water reuse projects or in agricultural runoff).



## INTRODUCTION

Among the photosensitizers present in the aquatic environment, nitrate and nitrite are often present at the highest concentrations, yet the extent to which they contribute to organic contaminant photodegradation is only partially understood. Absorption of sunlight by both nitrate and nitrite photochemically produces the hydroxyl radical ( $\cdot\text{OH}$ ), a nonselective oxidant.<sup>1–5</sup> However, under conditions typically encountered in surface waters, the scavenging of  $\cdot\text{OH}$  by organic matter,  $\text{HCO}_3^-$ , and  $\text{CO}_3^{2-}$  limits its importance to contaminant transformation to those compounds that are not susceptible to other transformation mechanisms.<sup>6</sup> Hydroxyl radical also reacts with nitrite to form nitrogen dioxide ( $\cdot\text{NO}_2$ ), a reactive nitrogen species.<sup>7</sup>  $\cdot\text{NO}_2$  and other reactive nitrogen species produced when nitrite or nitrate absorb light tend to be less susceptible to scavenging by organic matter and carbonate species<sup>8</sup> and therefore can contribute to transformation of organic contaminants under conditions in which steady-state  $\cdot\text{OH}$  concentrations would be extremely low due to scavenging by other solutes. For example, the presence of  $10\ \mu\text{M}$  nitrite in seawater increased the rate of phototransformation of phenol

by approximately four times despite the presence of numerous  $\cdot\text{OH}$  sinks.<sup>9</sup> The presence of similar concentrations of nitrite in cloudwater also has been shown to form nitrophenols through photochemical reactions involving dissolved nitrogen species and phenols.<sup>10,11</sup>

Nitrate- and nitrite-sensitized photolysis is of particular interest because these processes can result in the formation of nitrated and nitrosated transformation products that tend to be more toxic and persistent than their parent compounds. For example, nitrite-sensitized photolysis of phenol results in production of more toxic products, such as nitrosophenol and nitrophenol, while nitrate-sensitized photolysis forms nitrophenol.<sup>12–14</sup> Nitrite-sensitized photolysis also produces nitrated products of benzene and naphthalene.<sup>15,16</sup> Nitrated and nitrosated products of sulfamethoxazole and several  $\beta$ -blockers (e.g., atenolol, metoprolol) exhibit greater toxicity,

Received: March 5, 2019

Revised: April 30, 2019

Accepted: May 2, 2019

Published: May 13, 2019

mutagenicity, and carcinogenicity relative to the parent pharmaceutical compounds.<sup>17–22</sup> Relative to their parent compounds, nitro- and nitroso-transformation products tend to exhibit increased toxicity,<sup>23</sup> carcinogenicity,<sup>24–26</sup> and/or mutagenicity.<sup>27,28</sup> Nitration and nitrosation also alter the fate and transport of organic contaminants. For instance, nitrated products of sulfamethoxazole exhibit enhanced photostability relative to their parent compound.<sup>29</sup> The stability and toxicity of transformation products from reactions with reactive nitrogen species motivate the consideration of nitration and nitrosation pathways when photolysis occurs in the presence of nitrate and nitrite.

The relative importance of nitrate- and nitrite-photo-sensitized reactions to contaminant fate depends upon the concentrations of photosensitizers. Nitrate is typically present at concentrations ranging from 0.4 to 1.4 mM in nitrified municipal wastewater effluent and in effluent-dominated surface waters.<sup>30</sup> In agricultural runoff, nitrate is often present at concentrations up to 0.6 mM.<sup>6</sup> Nitrite tends to co-occur with nitrate, because it is produced during nitrification and denitrification.<sup>31</sup> Although the concentrations of nitrite are typically only 1–10% of those of nitrate, nitrite absorbs more sunlight than nitrate (its specific solar absorption rate is approximately 10 times greater than that of nitrate), making it a photosensitizer of similar importance to nitrate despite its lower concentrations.

To assess the relevance of nitrate and nitrite-sensitized photolysis in the aquatic environment, we studied the nitrate- and nitrite-sensitized photolysis of representative trace organic contaminants under environmentally relevant conditions. To gain insight into the reaction mechanisms and kinetics of these species, we focused our efforts on sulfamethoxazole, measuring its rate of transformation and the formation of a suite of transformation products. We used information from photolysis rates in the presence and absence of different radical scavengers to predict the relative importance of nitrate- and nitrite-sensitized photolysis under different conditions encountered in the aquatic environment. We also assessed the rates of nitrite-sensitized phototransformation of several trace organic compounds typically detected in municipal wastewater effluents to assess the relevance of this process to other contaminants.

## MATERIALS AND METHODS

**Materials.** Analytical reference standards of nitro-sulfamethoxazole and sulfamethoxazole-d<sub>4</sub>, and <sup>15</sup>N-labeled sodium nitrate and sodium nitrite were purchased from Toronto Research Chemicals (Toronto, Canada). Suwannee River natural organic matter (SRNOM) was obtained from the International Humic Substances Society. All other reagents and solvents were obtained from Fisher Scientific (Fairlawn, NJ). All solutions were prepared using deionized water from a Millipore water purification system.

**Phototransformation Experiments.** Photolysis experiments were conducted using an Oriel solar simulator (Spectra Physics 91194) equipped with a 1000 W Xe lamp and an atmospheric attenuation filter (Spectra Physics 81088 and 81017). Irradiance was verified at the start of each experiment with a spectroradiometer (Newport). A typical irradiance spectrum is provided in the Supporting Information (Figure S1). Experiments were carried out in 100 mL black-painted beakers containing 30 mL of the experimental solution, which were maintained at 20 ± 2 °C in a water bath. Subsamples (0.6

mL) from photolysis experiments were pipetted into 2 mL glass vials and stored at 4 °C prior to analysis, which occurred within 48 h.

**Kinetics Analysis.** Phototransformation rate constants were calculated from the slopes of linear regression of the natural logarithm of concentration versus time. Transformation rate constants for sulfamethoxazole (initial concentration = 2 μM) were quantified in the presence and absence of nitrite (NaNO<sub>2</sub>, 2 mM) and nitrate (NaNO<sub>3</sub>, 5 mM). The disappearance of sulfamethoxazole in the presence of nitrite or nitrate exhibited pseudo-first order kinetics under all conditions ( $r^2 > 0.93$ ).

Various control experiments were conducted to assess the impacts of experimental conditions on transformation rate constants. Experiments conducted in the dark indicated no sulfamethoxazole transformation, confirming that all removal was due to photochemical reactions. Removal rate constants were quantified in the presence of different buffers (5 mM phosphate buffer for pH 6–8, borate buffer pH 8–10). No differences in contaminant removal rate constants were observed for reactions in phosphate versus borate buffer at pH 8. Transformation rate constants were constant over a range of pH 6 to 10 in the presence of nitrite (Figure S2). Removal rate constants were also determined in the presence of dissolved inorganic carbon (0.4–4.2 mM, pH 6.0 and 10.0), Suwannee River natural organic matter (4–20 mg-C/L SRNOM), organic ·OH scavengers (10 or 100 mM tertiary butanol, isopropanol, ethanol, or methanol), and varying concentrations of inorganic nitrogen species (0.1–20 mM). The measured pH at the beginning and end of experiments did not change (± 0.3 pH units), indicating insignificant changes in inorganic carbon concentrations over the course of the experiments. A summary of rate constants observed in all experiments can be found in Table S2.

Transformation rate constants for other pharmaceuticals were assessed in 5 mM phosphate buffer at pH 7, in the presence of nitrite (2 mM), SRNOM (20 mg-C/L), and/or *tert*-butanol (250 mM). All kinetics experiments were conducted at an ionic strength of 25 mequiv/L, adjusted with sodium perchlorate.

**Transformation Product Identification.** To identify transformation products, 2 μM sulfamethoxazole was added to solutions buffered at pH 7 (5 mM phosphate buffer) and pH 10 (5 mM borate buffer). Nitrate or nitrite was added to buffer solutions using stock solutions of the sodium salts (5 mM final concentration). Tertiary butanol was added to some experiments as a ·OH scavenger. Transformation products were first detected by HPLC-MS/MS in full scan mode and then verified by both accurate mass and fragmentation patterns using high-resolution mass spectrometry in positive and negative ionization modes. To elucidate reaction mechanisms, some experiments were also carried out in the presence of <sup>15</sup>N-labeled nitrite and nitrate. Sodium salts of <sup>15</sup>NO<sub>2</sub><sup>-</sup> or <sup>15</sup>NO<sub>3</sub><sup>-</sup> were added to buffer solutions as described above, and changes in transformation product mass were investigated to determine incorporation of <sup>15</sup>N from reactive nitrogen species. Further method details for transformation product analysis are provided in the Supporting Information (S1.2).

To elucidate transformation products related to ·OH, hydrogen peroxide was added to some experiments at a final concentration of 2.5 mM in the absence of inorganic nitrogen

species. Rose bengal (40  $\mu\text{M}$ ) was used in other experiments as a source of singlet oxygen.

**Reverse Osmosis Concentrate Samples.** To validate the kinetic model and to assess transformation pathways under environmental conditions, experiments were conducted in samples of reverse osmosis (RO) concentrate produced from nitrified municipal wastewater effluent. Both nitrate (3.8 mM) and nitrite (87  $\mu\text{M}$ ) were present in the RO concentrate. Experiments were conducted in RO concentrate with and without the addition of 1 mM nitrite to determine the potential effect of incomplete denitrification in RO concentrate. The RO concentrate contained 35.5 mg-C/L dissolved organic matter and 11.7 mM dissolved inorganic carbon (pH = 7.6).

**Analytical Methods.** Sulfamethoxazole, additional pharmaceuticals, and transformation products were analyzed using an Agilent 1260 series HPLC coupled to an Agilent triple quadrupole tandem mass spectrometer (LC-MS/MS). Nitrite concentrations were determined using the Griess reagent method.<sup>32</sup> Further analytical method information is provided in the Supporting Information (S1.3–1.4).

## RESULTS AND DISCUSSION

**Kinetics of Nitrite-Sensitized Photolysis of Sulfamethoxazole.** The presence of nitrite or nitrate increased pseudo-first order rate constants for sulfamethoxazole transformation (Table S2) and resulted in the formation of unique transformation products, discussed below. Nitrite- and nitrate-sensitized photolysis results in the formation of several reactive intermediates which may have contributed to sulfamethoxazole transformation (1–4). First, in the nitrite absorption band centered around 350 nm, nitrite forms an excited state  $[\text{NO}_2^-]^*$ , which may react with organic contaminants via hydrogen abstraction.<sup>15,16</sup> In the absence of species that react with it,  $[\text{NO}_2^-]^*$  dissociates to  $\cdot\text{O}^-$  (which rapidly protonates to  $\cdot\text{OH}$  at circumneutral pH values) and nitric oxide (NO), which is oxidized to form nitrate in oxygen-containing solutions.<sup>7</sup> Nitrogen dioxide ( $\cdot\text{NO}_2$ ), which forms via reaction of  $\text{NO}_2^-$  with  $\cdot\text{OH}$ , reacts with organic compounds via electron transfer, H-abstraction, electrophilic addition, and substitution.<sup>33,34</sup>



To differentiate between the roles of  $\cdot\text{NO}_2$  and  $[\text{NO}_2^-]^*$  during sulfamethoxazole transformation, we observed changes in pseudo-first order reaction rate constants in the presence of hydroxyl radical scavengers. We used a series of organic scavengers (i.e., methanol, ethanol, isopropanol, and tertiary butanol) with known bimolecular reaction rate constants with  $\cdot\text{OH}$  (Figure S2) to verify the effect of  $\cdot\text{OH}$  scavenging. Reduction in transformation rates with the different scavengers were consistent with the reactivity of each scavenger with  $\cdot\text{OH}$ . Pseudo-first order sulfamethoxazole reaction rate constants were greatest in the presence of *t*-butanol, which has the lowest rate of reaction with  $\cdot\text{OH}$  and therefore the least inhibition, and were lowest for ethanol and isopropanol, which react most quickly with  $\cdot\text{OH}$ . Nonetheless, pseudo-first order rate

constants in nitrite-containing solutions were higher than predicted using rate constants for the reaction of  $\cdot\text{OH}$  with sulfamethoxazole and the scavengers. Furthermore, transformation products were detected which were not expected for reactions of sulfamethoxazole with  $\cdot\text{OH}$ , indicating that direct reaction of  $\cdot\text{OH}$  with sulfamethoxazole could not explain the observed reaction rates and products. The observation that  $\cdot\text{OH}$  scavengers lowered the sulfamethoxazole removal rate constant and slowed the formation of transformation products suggests that  $\cdot\text{NO}_2$ , rather than  $[\text{NO}_2^-]^*$ , was responsible for the increased transformation rate constants in the presence of nitrite.

Transformation rate constants in the presence of 2 mM nitrite were not affected at SRNOM concentrations ranging from 0 to 20 mg-C/L (Figure S2). Under these conditions, we predict that nearly all of the  $\cdot\text{OH}$  produced in 2 reacted with nitrite, with approximately 2% reacting with SRNOM. For the short light path lengths of the reactors used in our experiments (i.e.,  $\sim 2$  cm), the presence of 20 mg-C/L of natural organic matter screened out approximately 13% of the incident light at 350 nm (i.e., the wavelength of maximum absorption of nitrite), resulting in slower formation of nitrite-sensitized products (Figure S3). The observed removal rates of sulfamethoxazole were not affected by SRNOM, although light screening should have decreased the rate of direct photolysis by approximately 21% (see light screening calculations in SI Section 1.5). The absence of an observed effect of SRNOM on overall transformation rate constants indicates that organic matter-sensitized photolysis, perhaps via triplet-sensitized reactions or the production of reactive oxygen species,<sup>35</sup> compensated for the decrease in direct photolysis rates from light screening.

The presence of dissolved inorganic carbon increased pseudo-first order rate constants of nitrite-sensitized sulfamethoxazole phototransformation, due to formation of  $\cdot\text{CO}_3^-$ . On the basis of the reactivity of hydroxyl radical with nitrite and carbonate ( $k_{\text{OH},\text{NO}_2} = 10^{10}$ ;  $k_{\text{OH},\text{CO}_3} = 3.9 \times 10^8$ ,  $k_{\text{OH},\text{HCO}_3} = 8.9 \times 10^6$ ), we predict that more than 99% of the  $\cdot\text{OH}$  produced in reaction 2 reacted with nitrite. The formation of  $\cdot\text{CO}_3^-$  from the  $\cdot\text{OH}$  that reacted with carbonate increased the overall reaction rate constant by 5–37% (for inorganic carbon concentrations ranging from 0.4 to 4.2 mM) due to the selectivity of the carbonate radical. This effect was observed previously for indirect photolysis of sulfamethoxazole in wetland waters with elevated pH values<sup>36</sup> and is attributed to the high reactivity of  $\cdot\text{CO}_3^-$  with sulfur-containing functional groups.<sup>37</sup>

**Nitrite-Sensitized Transformation Products.** In experiments performed at pH 7.0 and 10.0 with 5 mM nitrite, three transformation products of sulfamethoxazole were detected: TP283, TP254, and TP299 (Figures 1 and 2). Transformation reactions occurred at the aromatic amine functional group.

TP283 was identified as 4-nitro-sulfamethoxazole by comparison of its HPLC-MS/MS retention time and fragmentation pattern with an analytical reference standard. TP283 was also formed from reactions of sulfamethoxazole with  $\cdot\text{OH}$  (produced by photolysis of  $\text{H}_2\text{O}_2$ ) and singlet oxygen (produced by photolysis of Rose Bengal), which is consistent with previous observations.<sup>18</sup> However, this transformation product was not detected in experiments conducted with 5–20 mg/L SRNOM in the absence of added inorganic nitrogen.

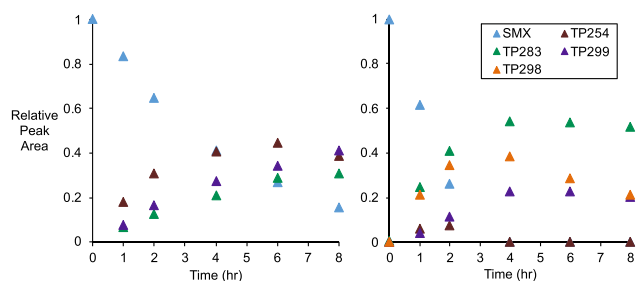


**Figure 1.** SMX removal and TP formation with 5 mM  $\text{NO}_2^-$  (left) or 5 mM  $\text{NO}_3^-$  (right) at pH 7 (5 mM phosphate buffer).

On the basis of exact mass calculations (Table S3), TP254 contains one more oxygen atom than sulfamethoxazole but is missing one nitrogen and one hydrogen atom, which is consistent with transformation of the aromatic amine to a phenolic functional group. This product has previously been observed as a minor product of direct photolysis (responsible for <1% of sulfamethoxazole transformation) when 100 mg/L of sulfamethoxazole was exposed to simulated sunlight.<sup>18</sup> In this study, its formation was not observed in photolysis experiments in the absence of inorganic nitrogen (i.e., it was not detected as a product of direct photolysis nor was it formed in the presence of hydrogen peroxide, Rose Bengal, or SRNOM) likely because it was produced at concentrations below the detection limit in our experiments with 2  $\mu\text{M}$  sulfamethoxazole.

Exact mass calculations indicate that TP299 contains three additional oxygen atoms relative to sulfamethoxazole, which is consistent with the presence of a hydroxyl and nitro group on the aromatic ring. This compound has not been previously reported and was only observed in the presence of inorganic nitrogen. TP299 could form either via hydroxylation of TP283 or via nitration of TP254. However, it is likely to be the product of TP254 nitration because its formation was not observed in experiments in which 5 mM nitrite was added to a 2  $\mu\text{M}$  solution of an analytical standard of 4-nitrosulfamethoxazole (i.e., TP283).

To further elucidate the role of reactive nitrogen species in the formation of TP283 and TP299, experiments were conducted using  $^{15}\text{NO}_2^-$ . Transformation products formed in photolysis experiments with  $^{15}\text{NO}_2^-$  exhibited  $m/z$  ratios for TP283 and TP299 that increased by one, indicating that the isotope-labeled nitrogen was incorporated into the transformation products. This finding indicates that TP283 was formed via substitution via an inorganic nitrogen species rather than by the oxidation of the amine group. While the oxidation of the aromatic amine groups to nitro groups has been

observed during ozonation,<sup>38</sup> to the best of our knowledge, the substitution of aromatic amine groups by nitro groups in the presence of reactive nitrogen species has not been reported previously.

The formation of these nitrite-sensitized transformation products was completely inhibited by the presence of 100 mM tertiary butanol but was only slightly affected by 20 mg-C/L of SRNOM (Figure S3), which is consistent with the kinetics results discussed earlier. The formation of the distinct products of nitrite-sensitized pathways in the presence of 20 mg-C/L SRNOM provides further evidence that the nitrite-sensitized reactive intermediates responsible for the transformation may be relevant to contaminant fate in the presence of organic matter.

**Kinetics of Nitrate-Sensitized Photolysis.** The transformation of sulfamethoxazole in the presence of nitrate was inhibited by 5 mM *tert*-butanol and by SRNOM, which is consistent with  $\cdot\text{OH}$  acting as the main oxidant. These relatively low concentrations of *tert*-butanol had a greater effect on nitrate-sensitized rate constants than they did in the nitrite system because nitrate is not an important sink for  $\cdot\text{OH}$ . At NOM concentrations of 4 mg-C/L and higher, photolysis rate constants when 5 mM  $\text{NO}_3^-$  was present decreased by more than 70% relative to experiments conducted in the absence of SRNOM. Experiments conducted at varying concentrations of dissolved inorganic carbon at pH 6 and pH 10 indicated that the sulfamethoxazole transformation rate constant was slightly higher in the presence of bicarbonate and much higher in the presence of carbonate relative to when dissolved inorganic carbon was absent (Figure S2), as predicted on the basis of previously developed photochemical models that account for the reactions of carbonate species with sulfamethoxazole.

These data suggest that reactive intermediates other than  $\cdot\text{OH}$  formed during nitrate photolysis are relatively unimportant to sulfamethoxazole transformation. Although  $\cdot\text{NO}_2$  is a product of nitrate photolysis and could be expected to contribute to nitrate-sensitized photolysis, the rate of formation of  $\cdot\text{NO}_2$  in the presence of 5 mM nitrate is only about 4% of its rate of formation in the presence of 2 mM nitrite. As a result, its contribution to transformation rates is expected to be negligible.

**Nitrate-Sensitized Transformation Products.** In the presence of nitrate at pH 7, all three sulfamethoxazole transformation products observed during nitrite-sensitized photolysis were observed as well as a product not observed during nitrite experiments: TP298. Exact mass calculations and fragmentation patterns suggest that TP298 is a direct nitration product of sulfamethoxazole, with the  $\text{NO}_2$  group adding to one of the carbons on the aromatic ring. During nitrate

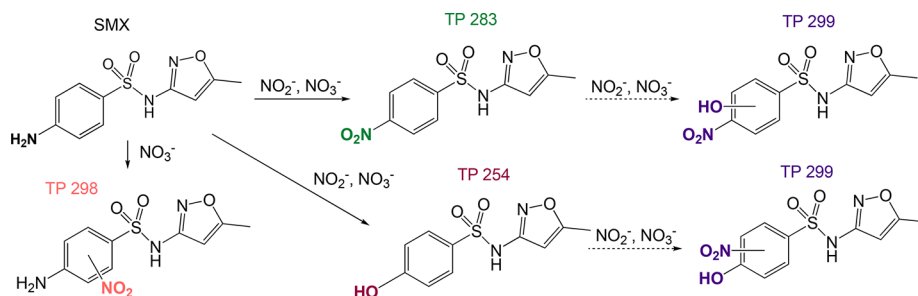


**Figure 2.** Proposed transformation product pathway for sulfamethoxazole in the presence of nitrite and nitrate.

photolysis, TP283 was formed by the direct oxidation of the amine group, as indicated by the results of the experiments conducted with isotope-labeled nitrate ( $^{15}\text{NO}_3^-$ ). TP254 was a minor product in the presence of nitrate, with much lower yields than those observed in the presence of nitrite. No mass shift was observed for TP299 formed in the presence of  $^{15}\text{NO}_3^-$ , indicating that TP299 is formed via the hydroxylation of TP283 during nitrate photolysis. The formation of TP283 and TP299 via oxidation and hydroxylation rather than nitration is consistent with  $\cdot\text{OH}$  serving as the oxidant.

To understand the mechanism of TP298 formation, the formation of reactive nitrogen species from nitrate needs to be considered. Nitrate photolysis produces  $\cdot\text{NO}_2$ , which has previously been observed to act as a nitrating agent in reactions with phenol.<sup>12</sup> However,  $\cdot\text{NO}_2$  is unlikely to be responsible for TP298 formation because TP298 was only observed in the presence of nitrate. Instead, TP298 may form through the reaction of sulfamethoxazole with peroxyxynitrite, a potent nitrating agent that is produced when  $\cdot\text{NO}_2$  and  $\cdot\text{OH}$  undergo recombination within the solvent cage during nitrate photolysis.<sup>7,39</sup> Nitrate photolysis also produces nitrite in a parallel reaction pathway with similar quantum yield to  $\cdot\text{NO}_2$  ( $\Phi \sim 0.01$ ).<sup>32</sup> However, in a nitrate-sensitized system, the contribution of nitrite-sensitized reactive intermediates is insignificant compared to the formation of  $\cdot\text{NO}_2$  and  $\cdot\text{OH}$  directly from nitrate.

**Nitrite-Sensitized Photolysis of Other Trace Organic Contaminants.** To assess the potential contribution of nitrite to the phototransformation of other trace organic contaminants, experiments were conducted with pharmaceuticals commonly detected in municipal wastewater effluent (Figure S4). Indirect phototransformation rate constants ( $k_{\text{indirect}}$ ) were calculated as the difference between observed transformation rates in the presence and absence of photosensitizers and were corrected for light screening. No removal was observed for compounds known to undergo slow direct and indirect photolysis (i.e., compounds that are only phototransformed via reaction with  $\cdot\text{OH}$ ): acyclovir, carbamazepine, atenolol, and metoprolol (data not shown). For several compounds, indirect phototransformation rate constants were higher in the presence of nitrite (Figure 3).

In the presence of 250 mM *t*-butanol, indirect phototransformation rate constants decreased by 34–51%. Under these conditions, we predict that approximately 98% of the  $\cdot\text{OH}$  reacted with the scavenger, which results in an 86% decrease in  $[\cdot\text{NO}_2]_{\text{ss}}$ . The observation that indirect transformation rate constants only decreased by 34–51% suggests that another indirect transformation pathway, in which  $\cdot\text{OH}$  is not involved, is partially responsible for the transformation of these compounds. At the elevated *t*-butanol concentrations used here, it is possible that the *tert*-butoxyl radical formed when  $\cdot\text{OH}$  is scavenged may contribute to contaminant removal. However, in experiments discussed above with sulfamethoxazole, the observed rate constants were lower than predicted, and not higher, in the presence of 100 mM *t*-butanol, indicating that the *t*-butoxyl radical did not increase reaction rate constants for sulfamethoxazole.

An alternative explanation for the effect of *t*-butanol on indirect transformation rate constants involves reactions of the compounds with  $[\text{NO}_2^-]^*$ , which forms before dissociation into NO and  $\cdot\text{OH}$ . The participation of this species in nitrite-sensitized photolysis was proposed previously as an explan-

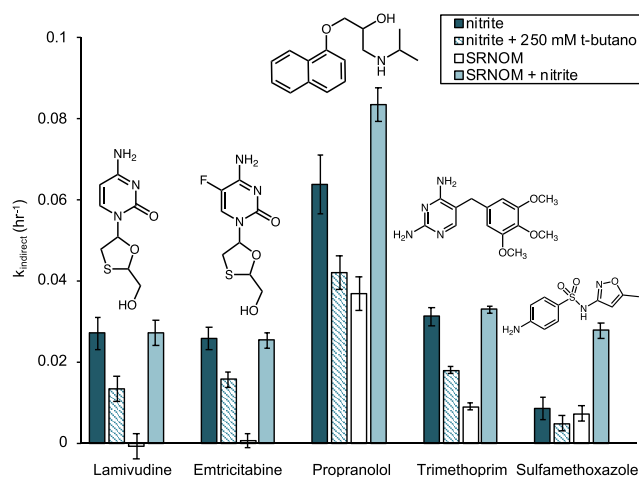


**Figure 3.** Indirect phototransformation rate constants of pharmaceuticals in 5 mM phosphate buffer solution, pH 7. Nitrite and SRNOM were added at concentrations of 2 mM and 20 mg-C/L, respectively. Error bars represent 95% confidence intervals obtained from linear regressions.

ation for the failure of isopropanol to slow the nitrite-sensitized transformation of naphthalene and benzene.<sup>15,16</sup>

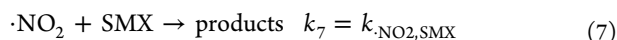
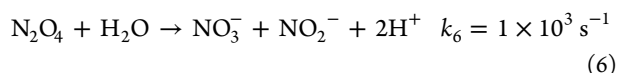
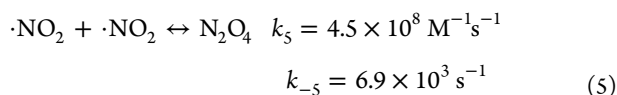
Propranolol and trimethoprim exhibited organic matter-sensitized photolysis in the absence of nitrite (20 mg-C/L SRNOM). When 2 mM nitrite was added in addition to organic matter, indirect photolysis rate constants of propranolol increased by an amount comparable to that observed when nitrite was present in the absence of organic matter, indicating that nitrite-sensitized photolysis was not affected by the presence of SRNOM. Conversely, for trimethoprim, the increase in the transformation rate constant observed in the presence of nitrite and SRNOM was about 18% less than the sum of nitrite- and SRNOM-sensitized rates. Interestingly, each of the compounds for which nitrite-sensitized photolysis was observed contains a primary amine attached to an aromatic or conjugated ring, except for propranolol (which contains an aliphatic secondary amine). This finding suggests that the amine moiety may be a reactive site for nitrite-sensitized photolysis, perhaps via H-abstraction by the reactive nitrogen species. Density functional theory calculations suggest that  $\cdot\text{NO}_2$  tends to react with aromatic compounds through hydrogen abstraction.<sup>40,41</sup> However, further research on transformation products is required to determine whether the amine moiety is the sole reaction site for nitrite-sensitized phototransformation of these compounds.

**Kinetic Model.** Although existing photochemical models accurately predict transformation kinetics for direct photolysis and indirect photolysis in the presence of organic matter and nitrate, an additional approach is needed to include the effects of nitrite. Nitrite-sensitized photolysis can occur via the reaction of organic contaminants either with  $\cdot\text{OH}$  or with  $\cdot\text{NO}_2$ . The approach for calculating the contribution of  $\cdot\text{OH}$  reactions to the overall transformation rate constant is the same as that used for nitrate-sensitized photolysis (equations provided in SI Section 2.5). We can model contaminant transformation rate constants due to  $\cdot\text{NO}_2$  as

$$k'_{\text{SMX},\text{NO}_2} = k_{\cdot\text{NO}_2,\text{SMX}}[\cdot\text{NO}_2]_{\text{ss}}$$

where  $[\cdot\text{NO}_2]_{\text{ss}}$  is the steady-state concentration of  $\cdot\text{NO}_2$  and  $k_{\cdot\text{NO}_2,\text{SMX}}$  is the bimolecular rate constant for the reaction between  $\cdot\text{NO}_2$  and sulfamethoxazole.

Under our experimental conditions,  $\cdot\text{NO}_2$  is primarily lost via 5–7.<sup>8</sup>



We calculated  $[\cdot\text{NO}_2]_{\text{ss}}$  according to equation S10 (SI Section 2.5) and performed a linear regression of  $k_{\cdot\text{NO}_2}$  (equal to light screening-corrected  $k_{\text{observed}} - k_{\text{direct}} - k_{\text{OH}}$  in experiments with sulfamethoxazole and varying nitrite concentrations at constant ionic strength) versus our calculated  $[\cdot\text{NO}_2]_{\text{ss}}$  to estimate a value for  $k_{\cdot\text{NO}_2,\text{SMX}}$  (Figure 4).

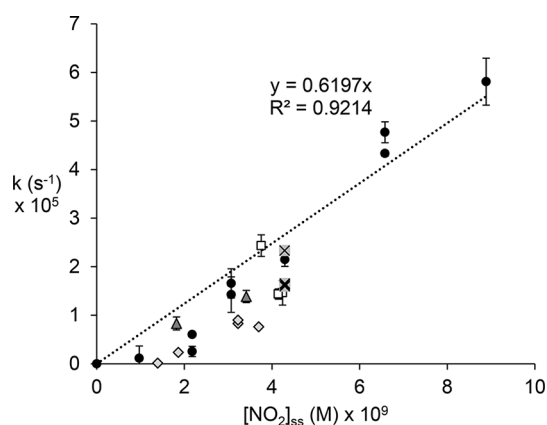


**Figure 4.** Linear regression of nitrite-sensitized reaction rate constants versus nitrogen dioxide steady-state concentration. Filled circles are included in regression analysis (experiments with only nitrite and SMX); open squares and gray triangles are rate constants observed in the presence of organic matter and in RO concentrate, respectively; gray diamonds and black X's are rate constants in the presence of organic scavengers and inorganic carbon, respectively, for comparison with model results.

We have also included rate constants attributed to nitrite-sensitized photolysis in the presence of SRNOM, dissolved inorganic carbon (0.40–4.2 mM bicarbonate or 0.40 mM carbonate), organic compounds used as radical scavengers (*tert*-butanol, methanol, ethanol, isopropanol), and solutes present in reverse osmosis concentrate in Figure 4. For experiments containing SRNOM or RO concentrate, the rate constants for nitrite-sensitized reactions were calculated by subtracting the modeled rate constants for organic matter-sensitized photolysis via singlet oxygen and  $\cdot\text{OH}$ . Values for the quantum yields of  $\cdot\text{OH}$  and singlet oxygen and for  $k_{\text{OH},\text{DOM}}$  were taken from Jasper and Sedlak<sup>36</sup> who modeled organic matter-sensitized reactions of these compounds in municipal wastewater. Despite known differences in photosensitizing and radical quenching properties between SRNOM and effluent organic matter,<sup>42,43</sup> experiments conducted in phosphate-buffered SRNOM solutions in the absence of inorganic nitrogen yielded rate constants comparable to those predicted

by this model ( $k_{\text{modeled}} = k_{\text{observed}}$ ). For experiments in solutions containing dissolved inorganic carbon, the contribution to reaction rate constants due to carbonate radical were subtracted from indirect phototransformation rate constants to estimate the contribution of nitrogen dioxide. At higher carbonate concentrations (i.e., 1.7 or 4.2 mM) observed rate constants were almost entirely attributable to carbonate radical, ( $k_{\cdot\text{NO}_2} \sim 0$ ) and were not included in Figure 4. The calculated bimolecular rate constant is given in Table 1 and is similar in magnitude to previously measured rate constants for reactions of  $\cdot\text{NO}_2$  with phenol and 4-chlorophenol.

**Table 1.** Bimolecular Rate Constants for Reactions with  $\cdot\text{NO}_2$

Compound	$k_{\cdot\text{NO}_2,\text{compound}}$ ( $\text{M}^{-1} \text{ s}^{-1}$ )
Phenol <sup>8</sup>	$3.2 \times 10^3$
4-Chlorophenol <sup>41</sup>	$1.1 \times 10^4$
Sulfamethoxazole	$6.2 \times 10^3$
Lamivudine	$6.2 \times 10^2$
Emtricitabine	$5.9 \times 10^2$
Propranolol	$1.5 \times 10^3$
Trimethoprim	$7.2 \times 10^2$

This modeling approach for nitrogen dioxide as the reactive intermediate was extended to the other wastewater-derived contaminants for which nitrite-sensitized photolysis was observed (i.e., propranolol, emtricitabine, trimethoprim, and lamivudine). Rate constants for these compounds were calculated from experiments conducted in the presence of 2 mM nitrite and are provided in Table 1. Very few rate constants for reaction with  $\cdot\text{NO}_2$  are available in the literature. However, our calculated values are similar in magnitude to rates previously measured for phenol<sup>8</sup> and chlorophenol<sup>41</sup> and slower than rates measured for phenolates, dimethylaniline ( $k = 2.6 \times 10^7$ ), and phenylenediamine ( $k = 4.6 \times 10^7$ ).<sup>33</sup>

**Photolysis Rates and Product Formation in RO Concentrate.** The  $\cdot\text{NO}_2$  modeling approach described in the previous section and the phototransformation models for nitrate and organic matter-sensitized photolysis described previously (summarized in SI Section 2.5)<sup>36</sup> were used to predict the relative importance of nitrate, nitrite, and organic matter in the photosensitized transformation of five representative trace organic contaminants. Among the different scenarios in which nitrite-sensitized sunlight photolysis could be important, the discharge of reverse osmosis concentrate from municipal water recycling programs is particularly relevant because it represents a situation where both nitrite and trace organic contaminants are present at elevated concentrations. To assess the relative importance of nitrite-sensitized photolysis, we considered a gradient of dilution representative of RO concentrate being released to surface water (Figure 5). Nitrate, nitrite, and pH values were based on concentrations measured in RO concentrate from a potable water reuse facility. For each contaminant, the relative importance of nitrite-sensitized photolysis was greatest prior to dilution. For sulfamethoxazole, indirect photolysis driven by nitrite accounts for 83% of transformation in undiluted RO concentrate. As the RO concentrate mixes with the receiving water, direct photolysis and DOM- and nitrate-sensitized reactions become more important. The contribution of nitrite includes reactions of the target contaminants with nitrogen dioxide and with hydroxyl radical produced by nitrite

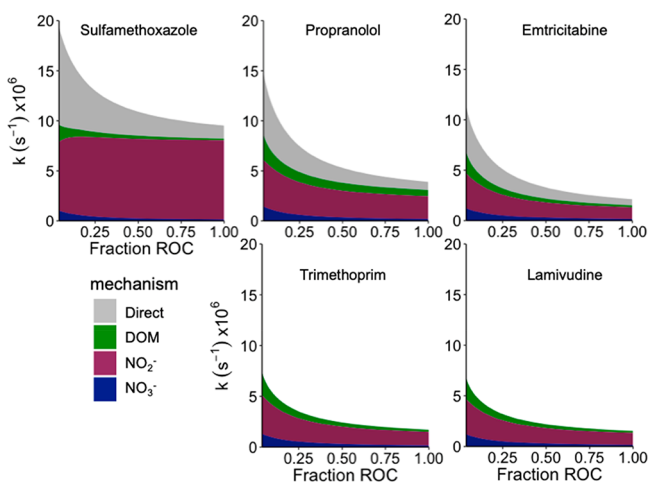


**Figure 5.** Modeled phototransformation rates of trace organic contaminants due to direct photolysis and indirect photolysis sensitized by dissolved organic matter (DOM), nitrate, or nitrite, as a function of ROC fraction (from dilute to 100% ROC). ROC: [DIC] = 120 mg-C/L, [DOC] = 50 mg-C/L, [NO<sub>3</sub><sup>-</sup>] = 5 mM, [NO<sub>2</sub><sup>-</sup>] = 0.5 mM. Receiving water: [DIC] = 5 mg-C/L, [DOC] = 2 mg-C/L, [NO<sub>3</sub><sup>-</sup>] = 0.1 mM, [NO<sub>2</sub><sup>-</sup>] = 0.01 mM.

photolysis. Reactions of sulfamethoxazole with  $\cdot\text{OH}$  are unimportant in undiluted RO concentrate due to  $\cdot\text{OH}$  scavenging by nitrite. Conversely, reactions with nitrogen dioxide are most important where nitrite concentrations are highest (i.e., in undiluted RO concentrate). For the other contaminants, the relative importance of nitrite-sensitized phototransformation depends on the bimolecular rate constants for reaction with  $\cdot\text{OH}$  versus with  $\cdot\text{NO}_2$ . In the case of sulfamethoxazole, reactions with  $\cdot\text{NO}_2$  account for 62–95% of the nitrite-sensitized rate constants, resulting in a decrease in the observed reaction rate constant as the RO concentrate is diluted. For the other organic contaminants, the predicted bimolecular reaction rate constants for reaction with  $\cdot\text{NO}_2$  are lower, such that the reactions with  $\cdot\text{OH}$  account for 22–35% of the nitrite-sensitized reactions in undiluted RO concentrate and 79–88% when the RO concentrate has been diluted to the point where it accounts for less than 5% of the overall flow.

Photolysis experiments performed in authentic RO concentrate were consistent with these predictions. The gray triangles in Figure 4 represent the sulfamethoxazole transformation rate constants observed in RO concentrate with and without added nitrite. In both cases, the observed rate constants agreed well with the predictions made with the nitrite-sensitized kinetic model. In addition, all of the products of the nitrite-sensitized reactions were observed in RO concentrate (which contained 35.5 mg-C/L organic carbon and 11.7 mM inorganic carbon) amended with 1 mM nitrite (Figure 6) indicating that the nitrite-sensitized pathways occur in authentic RO concentrate. The formation of TP298 was also observed in RO concentrate and is attributed to nitrate-sensitized pathways because it was not observed in the experiments containing only nitrite. TP298 formation was inhibited in the presence of SRNOM but occurred in nitrite-spiked RO concentrate, indicating that nitrate likely played a role in the sensitized photolysis in RO concentrate despite an overall small contribution to removal rates. TP formation was not observed to an appreciable degree in RO concentrate without added nitrite, likely due to the low

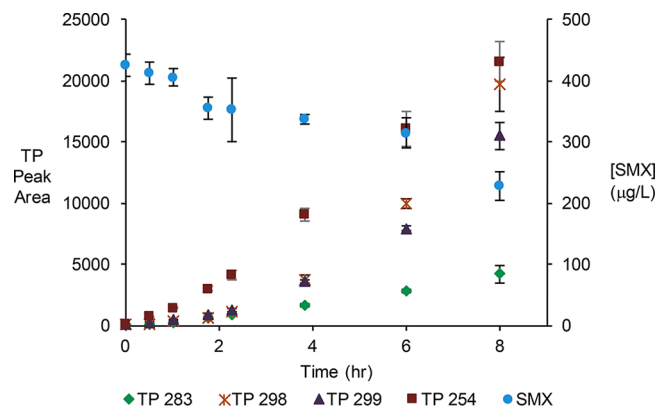


**Figure 6.** SMX removal and transformation product (TP) formation in RO concentrate amended with 1 mM nitrite. Ionic strength = 0.2 M; pH = 7.6; [NO<sub>3</sub><sup>-</sup>] = 3.8 mM; [NO<sub>2</sub><sup>-</sup>] = 1.3 mM; [DIC] = 11.7 mM; [DOC] = 35 mg-C/L.

concentration of nitrite in the particular RO concentrate sample used in these experiments.

In the specific case of discharging RO concentrate, we predict that dilution with receiving waters that do not contain elevated concentrations of DOM increases photolysis rates, via direct photolysis and DOM- or nitrate-sensitized reactions, and decreases the rates and relative importance of the nitrogen dioxide reaction pathway, which may lead to undesirable products. It is worth noting that biological treatment of the RO concentrate could be used as a means of increasing nitrite concentrations (e.g., through partial denitrification) prior to sunlight exposure. In this case, the elevated nitrite concentrations would likely contribute to faster organic contaminant removal via nitrite-sensitized photolysis. However, the formation of nitrated transformation products (e.g., TP299) might be a concern under this scenario.

The nitrite-sensitized reactions could also occur during wetland treatment or the discharge of nitrified wastewater effluent or in pesticide-contaminated agricultural runoff which flows through drainage channels exposed to sunlight. In the presence of 0.1 mM nitrite, our model indicates that nitrite-sensitized reactions would account for 69% of sulfamethoxazole transformation and 89 and 58% of lamivudine and propranolol phototransformation, respectively, in sunlit wastewater (5 mg-C/L DOC, 2.5 mM DIC, 1 mM NO<sub>3</sub><sup>-</sup>, pH 7). In agricultural runoff, 80, 92, and 64% of phototransformation would be attributable to nitrite-sensitized reactions for sulfamethoxazole, lamivudine, and propranolol, respectively (0.2 mM NO<sub>2</sub><sup>-</sup>, 20 mg-C/L DOC, 1 mM DIC, 0.5 mM NO<sub>3</sub><sup>-</sup>, pH 7). Agricultural runoff may not contain significant concentrations of these pharmaceuticals, but it may contain pesticides with functional groups susceptible to the same nitrite-sensitized phototransformation pathways (e.g., primary and secondary amines). Direct photolysis may be faster in these matrices due to less light screening, making the relative contribution of nitrite less important than in the case of RO concentrate. However, the nitrite-sensitized contribution may still be significant, and the accumulation of nitrated and nitrosated products should be considered in cases where photolysis occurs in the presence of nitrite.

## ■ ASSOCIATED CONTENT

### ■ Supporting Information

The Supporting Information is available free of charge on the ACS Publications website at DOI: 10.1021/acs.est.9b01386.

Setup of the solar simulator, analysis of trace organic contaminants and transformation products, nitrite analysis and light screening calculations, detailed data on contaminant transformation kinetics, effects of organic matter on kinetics, results of high-resolution mass spectrometry analysis, kinetics of transformation of additional compounds and the kinetic model for nitrogen dioxide (PDF)

## ■ AUTHOR INFORMATION

### Corresponding Author

\* E-mail: [sedlak@berkeley.edu](mailto:sedlak@berkeley.edu).

### ORCID

Rachel C. Scholes: 0000-0001-5450-8377

Carsten Prasse: 0000-0002-1470-141X

David L. Sedlak: 0000-0003-1686-8464

### Present Address

<sup>§</sup>Department of Environmental Health and Engineering, Johns Hopkins University, Baltimore Maryland, 21218 United States.

### Notes

The authors declare no competing financial interest.

## ■ ACKNOWLEDGMENTS

This research was supported by the National Science Foundation (NSF), through the Engineering Research Center for Reinventing the Nation's Urban Water Infrastructure (ReNUWI; EEC-1028968) and a NSF Graduate Research Fellowship, and by the Department of Energy, through the Clean Energy Research Center for Water Energy Technologies (CERC-WET). Additional support and samples of RO concentrate were provided by Santa Clara Valley Water District through the Reverse Osmosis Concentrate Management Project.

## ■ REFERENCES

- (1) Zepp, R. G.; Hoigné, J.; Bader, H. Nitrate-induced photo-oxidation of trace organic-chemicals in water. *Environ. Sci. Technol.* **1987**, *21* (5), 443–450.
- (2) Zafiriou, O. C.; True, M. B. Nitrate photolysis in seawater by sunlight. *Mar. Chem.* **1979**, *8* (1), 33–42.
- (3) Zafiriou, O. C.; True, M. B. Nitrite photolysis in seawater by sunlight. *Mar. Chem.* **1979**, *8* (1), 9–32.
- (4) Vaughan, P. P.; Blough, N. V. Photochemical formation of hydroxyl radical by constituents of natural waters. *Environ. Sci. Technol.* **1998**, *32* (19), 2947–2953.
- (5) Mopper, K.; Zhou, X. Hydroxyl radical photoproduction in the sea and its potential impact on marine processes. *Science* **1990**, *250*, 661–664.
- (6) Brezonik, P. L.; Fulkerson-Brekken, J. Nitrate-induced photolysis in natural waters: Controls on concentrations of hydroxyl radical photo-intermediates by natural scavenging agents. *Environ. Sci. Technol.* **1998**, *32*, 3004–3010.
- (7) Mack, J.; Bolton, J. Photochemistry of nitrite and nitrate in aqueous solution: a review. *J. Photochem. Photobiol., A* **1999**, *128*, 1–13.
- (8) Minero, C.; Chiron, S.; Falletti, G.; Maurino, V.; Pelizzetti, E.; Ajassa, R.; Carlotti, M. E.; Vione, D. Photochemical processes involving nitrite in surface water samples. *Aquat. Sci.* **2007**, *69*, 71–85.

(9) Calza, P.; Vione, D.; Novelli, A.; Pelizzetti, E.; Minero, C. The role of nitrite and nitrate ions as photosensitizers in the photo-transformation of phenolic compounds in seawater. *Sci. Total Environ.* **2012**, *439*, 67–75.

(10) Harrison, M. A.J.; Barra, S.; Borghesi, D.; Vione, D.; Arsene, C.; Olariu, R. I. Nitrated phenols in the atmosphere: a review. *Atmos. Environ.* **2005**, *39*, 231–248.

(11) Vione, D.; Maurino, V.; Minero, C.; Pelizzetti, E. New processes in the environmental chemistry of nitrite: nitration of phenol upon nitrite photoinduced oxidation. *Environ. Sci. Technol.* **2002**, *36* (4), 669–676.

(12) Vione, D.; Sur, B.; Dutta, B. K.; Maurino, V.; Minero, C. On the effect of 2-propanol on phenol photolysis upon nitrate photolysis. *J. Photochem. Photobiol., A* **2011**, *224*, 68–70.

(13) Vione, D.; Maurino, V.; Pelizzetti, E.; Minero, C. Phenol photolysis and photolysis upon nitrite photolysis in basic solution. *Int. J. Environ. Anal. Chem.* **2004**, *84* (6–7), 493–504.

(14) Machado, F.; Boule, P. Photolysis and photolysis of phenolic derivatives induced in aqueous solution by excitation of nitrite and nitrate ions. *J. Photochem. Photobiol., A* **1995**, *86*, 73–80.

(15) Vione, D.; Maurino, V.; Minero, C.; Lucchiari, M.; Pelizzetti, E. Nitration and hydroxylation of benzene in the presence of nitrite/nitrous acid in aqueous solution. *Chemosphere* **2004**, *56*, 1049–1059.

(16) Vione, D.; Maurino, V.; Minero, C.; Pelizzetti, E. Nitration and photolysis of naphthalene in aqueous systems. *Environ. Sci. Technol.* **2005**, *39*, 1101–1110.

(17) Osorio, V.; Sanchis, J.; Abad, J. L.; Ginebreda, A.; Farre, M.; Perez, S.; Barcelo, D. Investigating the formation and toxicity of nitrogen transformation products of diclofenac and sulfamethoxazole in wastewater treatment plants. *J. Hazard. Mater.* **2016**, *309*, 157–164.

(18) Gmurek, M.; Horn, H.; Majewsky, M. Phototransformation of sulfamethoxazole under simulated sunlight: Transformation products and their antibacterial activity toward *Vibrio fischeri*. *Sci. Total Environ.* **2015**, *538*, 58–63.

(19) Majewsky, M.; Wagner, D.; Delay, M.; Brase, S.; Yargeau, V.; Horn, H. Antibacterial activity of sulfamethoxazole transformation products (TPs): General relevance for sulfonamide TPs modified at the para position. *Chem. Res. Toxicol.* **2014**, *27*, 1821–1828.

(20) Martelli, A.; Allavena, A.; Sottofattori, E.; Brambilla, G. Low clastogenic activity in vivo of the N-nitroso derivatives of 5  $\beta$ -adrenergic-blocking drugs proved to be potent genotoxins in vitro. *Toxicol. Lett.* **1994**, *73* (3), 185–191.

(21) Robbiano, L.; Martelli, A.; Allavena, A.; Mazzei, M.; Gazzaniga, G. M.; Brambilla, G. Formation of the N-nitroso derivatives of six  $\beta$ -adrenergic-blocking agents and their genotoxic effects in rat and human hepatocytes. *Cancer Res.* **1991**, *51*, 2273–2279.

(22) Toolaram, A. P.; Menz, J.; Rastogi, T.; Leder, C.; Kummerer, K.; Schneider, M. Hazard screening of photo-transformation products from pharmaceuticals: Application to selective  $\beta_1$ -blockers atenolol and metoprolol. *Sci. Total Environ.* **2017**, *579*, 1769–1780.

(23) Chen, P.; Lv, W.; Chen, Z.; Ma, J.; Li, R.; Yao, K.; Liu, G.; Li, F. Phototransformation of mefenamic acid induced by nitrite ion in water: mechanism, toxicity, and degradation pathways. *Environ. Sci. Pollut. Res.* **2015**, *22*, 12585–12596.

(24) Dai, N.; Mitch, W. A. Relative importance of N-nitrosodimethylamine compared to total N-nitrosamines in drinking waters. *Environ. Sci. Technol.* **2013**, *47*, 3648–3656.

(25) d'Ischia, M.; Napolitano, A.; Manini, P.; Panzella, L. Secondary targets of nitrite-derived reactive nitrogen species: nitrosation/nitration pathways, antioxidant defense mechanisms and toxicological implications. *Chem. Res. Toxicol.* **2011**, *24*, 2071–2092.

(26) Jakszyn, P.; Gonzalez, C. A. Nitrosamine and related food intake and gastric and oesophageal cancer risk: A systematic review of the epidemiological evidence. *World J. Gastroenterol.* **2006**, *12* (27), 4296–4303.

(27) Kovacic, P.; Somanathan, R. Nitroaromatic compounds: Environmental toxicity, carcinogenicity, mutagenicity, therapy and mechanism. *J. Appl. Toxicol.* **2014**, *34* (8), 810–824.



(28) Purohit, V.; Basu, A. K. Mutagenicity of nitroaromatic compounds. *Chem. Res. Toxicol.* **2000**, *13* (8), 673–692. Dai, N.; Mitch, W. A. Relative importance of *N*-nitrosodimethylamine compared to total *N*-nitrosamines in drinking waters. *Environ. Sci. Technol.* **2013**, *47*, 3648–3656.

(29) Bonvin, F.; Omlin, J.; Rutler, R.; Schweizer, W. B.; Alaimo, P. J.; Strathmann, T. J.; McNeill, K.; Kohn, T. Direct photolysis of human metabolites of the antibiotic sulfamethoxazole: evidence for abiotic back-transformation. *Environ. Sci. Technol.* **2013**, *47* (13), 6746–6755.

(30) Pocerlich, M.; Litke, D. W. Nutrient concentrations in wastewater treatment plant effluents, South Platte River basin. *J. Am. Water Resour. Assoc.* **1997**, *33* (1), 205–214.

(31) Alleman, J. E. Elevated nitrite occurrence in biological wastewater treatment systems. *Water Sci. Technol.* **1985**, *17*, 409–419.

(32) Benedict, K. B.; McFall, A. S.; Anastasio, C. Quantum yield of nitrite from the photolysis of aqueous nitrate above 300 nm. *Environ. Sci. Technol.* **2017**, *51* (8), 4387–4395.

(33) Huie, R.; Neta, P. Kinetics of one-electron transfer reaction involving  $\text{ClO}_2$  and  $\text{NO}_2$ . *J. Phys. Chem.* **1986**, *90*, 1193–1198.

(34) Ji, Y.; Wang, L.; Jian, M.; Lu, J.; Ferronato, C.; Chovelon, J.-M. The role of nitrite in sulfate radical-based degradation of phenolic compounds: An unexpected nitration process relevant to groundwater remediation by *in-situ* chemical oxidation (ISCO). *Water Res.* **2017**, *123*, 249–257.

(35) Bahnmüller, S.; von Gunten, U.; Canonica, S. Sunlight-induced transformation of sulfadiazine and sulfamethoxazole in surface waters and wastewater effluents. *Water Res.* **2014**, *57*, 183–192.

(36) Jasper, J. T.; Sedlak, D. L. Phototransformation of wastewater-derived trace organic contaminants in open-water unit process treatment wetlands. *Environ. Sci. Technol.* **2013**, *47* (19), 10781–10790.

(37) Chen, S.; Hoffman, M. Z. Effect of pH on the reactivity of the carbonate radical in aqueous solution. *Radiat. Res.* **1975**, *62* (1), 18–27.

(38) von Sonntag, C.; von Gunten, U. *Chemistry of Ozone in Water and Wastewater Treatment: From Basic Principles to Applications*. IWA Publishing: London, UK, 2012.

(39) Huang, Y.; Kong, M.; Westerman, D.; Xu, E. G.; Coffin, S.; Cochran, K. H.; Liu, Y.; Richardson, S. D.; Schlenk, D.; Dionysiou, D. D. Effects of  $\text{HCO}_3^-$  on Degradation of Toxic Contaminants of Emerging Concern by UV/ $\text{NO}_3^-$ . *Environ. Sci. Technol.* **2018**, *52*, 12697–12707.

(40) Ceron-Carrasco, J. P.; Bastida, A.; Zúñiga, J.; Requena, A.; Miguel, B. A theoretical study of the reaction of *b*-carotene with the nitrogen dioxide radical in solution. *J. Phys. Chem. B* **2010**, *114* (12), 4366–4372.

(41) Bedini, A.; Maurino, V.; Minero, C.; Vione, D. Theoretical and experimental evidence of the photonation pathway of phenol and 4-chlorophenol: A mechanistic study of environmental significance. *Photochem. Photobiol. Sci.* **2012**, *11*, 418–424.

(42) Dong, M. M.; Rosario-Ortiz, F. L. Photochemical Formation of Hydroxyl Radical from Effluent Organic Matter. *Environ. Sci. Technol.* **2012**, *46* (7), 3788–3794.

(43) Haag, W. R.; Hoigné, J. Singlet Oxygen in Surface Water. 3. Photochemical Formation and Steady-State Concentrations in Various Types of Waters. *Environ. Sci. Technol.* **1986**, *20* (4), 341–348.